Improvement of the deep UV sensor performance of a β-Ga2O3 photodiode by coupling of two planar diodes

Vieira, Douglas H.; Badiei, Nafiseh; Evans, Jonathan E.; Alves, Neri; Kettle, Jeffrey; Li, Lijie

IEEE Transactions on Electron Devices

DOI:
https://doi.org/10.1109/TED.2020.3022341

Published: 01/11/2020

Peer reviewed version

Improvement of the deep UV sensor performance of a β-Ga_2O_3 photodiode by coupling of two planar diodes

Douglas H. Vieira, Nafiseh Badiei, Jonathan E. Evans, Neri Alves, Jeffrey Kettle, Lijie Li

Abstract — β-Ga_2O_3 is one of promising semiconductor materials that has been widely used in power electronics and ultraviolet (UV) detectors due to its wide bandgap and high sensitivity to UV light. Specifically, for the UV detection application, it has been reported that the photocurrent was in the scale of micro Amps (μA), which normally requires sophisticated signal processing units. In this work, a novel approach based upon coupling of two Schottky diodes is reported, leads to a substantial increase in photocurrent (~186 times) when benchmarked against a conventional planar UV photodiode. The detectivity and responsivity of the new device have also been significantly increased; the rectification ratio of this device was measured to be 1.7 x 10^7 with ultra-low dark current, when measured in the reverse bias. The results confirm the approach of coupling two Schottky diodes has enormous potential for improving the optical performance of deep UV sensors.

***Index Terms* — Gallium Oxide, Photodetector, Deep UV, Schottky Diode, Performance Improvement.**

I. INTRODUCTION

OVER the past 5 years, significant efforts has been conducted on new forms of ultraviolet (UV) photodiodes for a wide range of applications such as in the military, environmental, medical and industrial markets which require the sensor to operate in harsh situations [1]. The most common commercial UV photodiodes are Si-based, but these possess limited sensitivity at UV wavelengths [2]. Wide bandgap semiconductor materials, such as MgZnO and AlGaN, had been reported as an alternative to Si, but it remains a challenge to achieve good crystalline quality as a result of the heavy doping levels needed [3]. Gallium oxide (Ga_2O_3) stands out as an alternative material to UV photodiodes and has been the subject of intense recent research [4]. It can be manufactured with five crystallographic phases: α, β, γ, δ and ε, although the β phase (β-Ga_2O_3) has been the most used in electronic devices applications due to its chemical and thermodynamic stability [5]. Furthermore, β-Ga_2O_3 has a very large breakdown field (E_b) value and a wide bandgap, ~8 MV/cm and 4.9 eV [6], respectively. Therefore, it is a promising material for power electronics and its ability to handle high electrical fields is greatly advantageous for the reduction of device size and enhancement of the integration level of power modules [7]. Aiming to explore these advantageous properties, numerous devices have been reported using this material, for example: Schottky diodes [8], transistors [9], solar cells [10], gas sensors [5] and LEDs [11]. Most significantly, β-Ga_2O_3 has been used for deep UV sensing applications such as for solar-blinds [12] because it eliminates the need to use interference filters [13] and achieves high values of rejection ratio of visible light [14,15]. This material can also be applied to biomedical area, detection of corona discharge, UV curing of paints/adhesives, machine vision, monitoring UV exposure for skin cancer, forensics, flame and chemical sensing [16].

One of the major challenges for manufacturing β-Ga_2O_3 devices is to achieve a robust ohmic contact. This difficulty arises from the β-Ga_2O_3 surface due to the upward band

The work was supported by the Solar Photovoltaic Academic Research Consortium II (SPARC II) project, gratefully funded by WEFO.

J. Kettle is with the School of Electronic Engineering, Bangor University - Bangor, Wales, UK. (e-mail: j.kettle@bangor.ac.uk).

N. Badiei, J. E. Evans and L. Li, are with the Multidisciplinary Nanotechnology Centre, College of Engineering, Swansea University, Swansea, Wales, UK. (e-mail: n.badiei@swansea.ac.uk, j.e.evans@swansea.ac.uk and l.li@swansea.ac.uk, respectively).

D. H. Vieira and N. Alves are with the Departamento de Física, UNESP - São Paulo State University, Presidente Prudente, Brazil. (e-mail: douglas.vieira@unesp.br and neri.alves@unesp.br, respectively).

bending inducing electron depletion [17]. Yao *et al* reported Ti, In, Ag, Sn, W, Mo, Sc, Zn and Zr [18] as materials suitable for ohmic contacts. Higashiwaki *et al* reported the first *β*-Ga_2O_3 transistor using Ti/Au as an ohmic contact [6], but to achieve this condition it was necessary to use reactive ion etching (RIE) with a mixture of BCl_3 and Ar. Bae *et al* reported that this same Ti/Au contact also can be rectifier [19]. The latter reports that the contact properties are highly dependent on the atmosphere in which the material is annealed because the performance is dominated by the formation of oxygen vacancies. The barrier height also seems to be affected by the interface states and impurities [7]. It has been showed that moderate annealing (~400 ºC) improves the Ti/Au ohmic behavior [18] and also tends to yield higher ideality factors in diodes [20], that is related to the high barrier, but Carey *et al* reported that Ti/Au (20nm/80nm) can presents Schottky behavior even if annealed at 300 to 600 ºC [21]. The mixture of ohmic and Schottky contacts on the same material on the Ga_2O_3 may give rise to novel UV detecting devices with enhanced performances. Typically, it has been reported that the photocurrent of Ga_2O_3 based UV detectors are typically in the μA range [15], which is probably attributed to the fact that achieving highly conductive Ga_2O_3 is challenging.

In this work, we report the performance of a *β*-Ga_2O_3 Schottky diode in a planar architecture using Ti/Au as electrode for the ohmic and Schottky contact. This device showed promising properties both as a diode and as a deep UV photodetector. Moreover, we are able to dramatically improve the performance (photocurrent) by inclusion of a third Ti/Au electrode, resulting in a two-diode coupled device. The influence of voltage bias at this third electrode was studied and the device exhibited substantial enhancement of all figures of merit of photodetectors in comparison to the Schottky diode.

II. EXPERIMENTAL DETAILS

β-Ga_2O_3 (010) wafer with thickness of 0.5 mm and face polishing obtained by edge-defined film-fed growth (EFG) method was purchased from Tamura Corporation®. The substrate was grown with Sn as dopant at a concentration of $8.3x10^{18}$ cm^{-3}. The substrate was thoroughly cleaned using acetone, isopropanol and dried with nitrogen followed by placing them 10 minutes on 150 °C hotplate for complete dehydration. The contacts were patterned via a lift-off process. Samples were spin coated with 2 % PMMA 950K (EM Resists Ltd.) at 3000 rpm, exposed using electron beam lithography (EBL) at an acceleration voltage of 30 kV then developed using 1:3 MIBK:IPA. To form the electrical contacts, a 20 nm Ti layer followed by a 100 nm Au layer were deposited on the surface of β-Ga_2O_3 wafer using physical vapor deposition (PVD). **Fig. 1a** shows a picture of the device. After the electrode deposition, the sample was submitted to a rapid thermal annealing (RTA) at 400 ºC for 1 min in a N_2 atmosphere at a pressure of approximately 1 mbar. Although all the contacts pads were prepared on the sample concurrently, they do not all have the same characteristics; some are measured as Schottky and others as ohmic, due to the gradient of distribution of interface states and impurities at the film surface, which is a common problem in β-Ga_2O_3 devices.

Two types of devices were studied: 1) two-terminal devices, i.e a Schottky diode and 2) three-terminal device formed by the coupling of two Schottky diodes. The cross-section of both devices is presented at the **Fig 1b**, identifying which contacts are ohmic and Schottky. The photodetector form a planar structure with an active area of 0.02048 cm^2. An Agilent B2912A unit connected to a probe station was used to obtain current versus voltage (I–V) and current versus time (I–t) curves using it in the dark and deep UV (254 nm, 1.58 mW/cm^2), at room temperature and atmosphere. To calculate the photodetector figures of merit (FOM), the power density of the UV light was measured using a UV-enhanced photodiode purchased from Thorlabs (model FDS010).

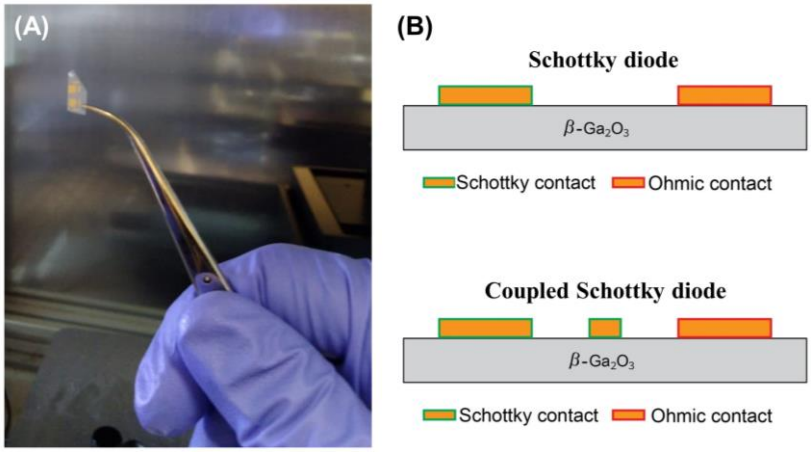

Fig 1. a) Photograph of the β-Ga_2O_3 device and b) diagram showing the cross-section of the β-Ga_2O_3 devices of the conventional Schottky diode (top) and coupled Schottky diode (below).

III. RESULTS AND DISCUSSION

A. Results of Schottky diode experiments

Fig. 2a presents the I−V characteristics of the β-Ga_2O_3 Schottky diode in the dark and under UV irradiation. In the dark, this curve presents a typical rectification behavior expected for Schottky diodes by the following equation:

$$I = AA^*T^2 \exp\left(-\frac{q\phi_B}{kT}\right)\left[\exp\left(\frac{qV_d}{nkT}\right) - 1\right] \quad (1)$$

where q is electron charge, ϕ_B is Schottky barrier height, V_d is applied voltage, k is Boltzmann constant, T is temperature, n is ideality factor, A is effective area and A^* is effective Richardson constant. This β-Ga_2O_3 Schottky diode exhibited good rectifying properties with a high rectification ratio of ($RR = I_{forward}/I_{reverse}$) $9.16x10^6$ between ± 10 V, a forward turn-on voltage of around 2 V and also a low current under reverse bias (~10^{-11} A). The series resistance (R_s) was calculated as 9.6 $k\Omega$ using the Cheung's method ($R_s = \frac{dV}{dlnI}\frac{q}{nkT}$) [22]; the large R_s is syntomic by the non-ideal Ti/β-Ga_2O_3 contact.

Under UV exposure (254 nm, 1.58 mW/cm^2), the photodiode exhibits a significant change in the current under reverse bias (see **Fig. 2**). To evaluate the performance of this device as a deep UV photodetector, figures of merit were calculated, in particular: responsivity (R_λ), external quantum efficiency (EQE), detectivity (D^*) and PDCR (photo to dark current ratio). The responsivity and EQE were estimated using equations 2 and 3, respectively:

$$R_\lambda = \frac{J_{ph}}{P_d}, \quad (2)$$

$$EQE(\%) = \frac{R_\lambda hc}{q\lambda} x100, \quad (3)$$

with J_{ph} being the photocurrent density, P_d the power density of the incident light, h the Planck's constant, c the speed of light and λ the exciting wavelength. The calculated values of responsivity and EQE were 0.0125 A/W and 6.12 %, respectively. Detectivity and PCDR were used to characterize the response of our sensors and were calculated using equations 4 and 5, respectively. Consequently, the calculated detectivity and PDCR of the Schottky diode was measured at 1.02x10^{12} Jones and 4.26x10^4, respectively.

$$D^* = \frac{R_\lambda}{\sqrt{2qJ_{dk}}}, \quad (4)$$

$$PDCR = \frac{I_{uv} - I_{dk}}{I_{dk}}, \quad (5)$$

From the results above, this diode exhibits sensing behaviour for deep UV detection, but it presents a poor responsivity, when compared to state-of-the-art performances in the literature. The likely reason for this is the imperfectness of the interface/junction between a β-Ga_2O_3 and the metal electrodes.

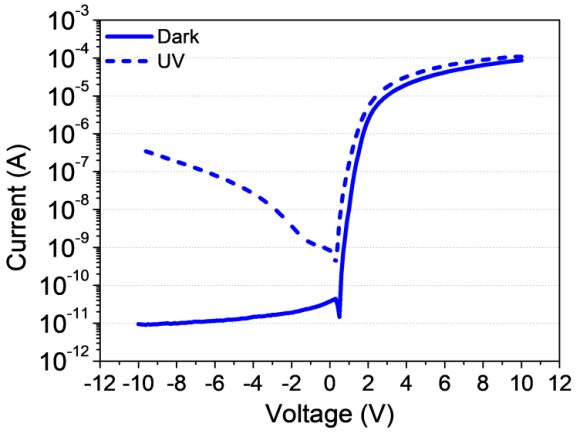

Fig. 2: I-V curves of the β-Ga_2O_3 Schottky diode in the dark and under UV light.

In the context of the next section, it is important to understand the physical mechanism for the generation of photocurrent in this device. Around the proximity of the Schottky contact in β-Ga_2O_3 devices, there are traps due to oxygen deficiency and, under deep UV exposure, the photogenerated pair disassociates, leading to the holes being trapped in the oxygen vacancies, preventing recombination with the electrons and increasing the depletion layer [23]. These mechanisms can be represented by the follow equation, where UV is the incident photon and V_o is an oxygen vacancy:

$$UV + V_o^0 \rightarrow V_o^{2+} + 2e^-. \quad (6)$$

The change in the charge concentration near the Schottky contact increases the internal electric field and lowers the effective Schottky barrier in the reverse bias, thus leading to an increase in the current [13]. Using the Cheung's method, it was calculated a lowing effect of 0.2 eV (the barrier changed from 0.94 eV in the dark to 0.74 eV under UV light).

B. Results of coupled Schottky diode experiments

In order to improve performance and achieve higher FOM values, the device was modified by coupling to a third Schottky electrode. In the inset of **Fig. 3a,** a schematic equivalent circuit is presented of this novel configuration. **Fig. 3a** shows the I−V characteristics of the coupled Schottky diode in dark, where the voltage level of the third electrode (V_{third}) is modified from 0 V to 9 V. The curves continue to show a typical rectification behavior expected for a Schottky diode and it also presents a high current of 2 mA in the forward bias. Moreover, when different levels of the third voltage was applied, it was possible to adjust the turn-on voltage, from around 2 V to around 7 V, although all curves reach approximately the same maximum current due to limitations in the bulk limited region. **Fig. 3b** shows that the turn-on voltage has a linear relationship with the voltage level at the third electrode.

Fig. 3c shows the I−V characteristics of the coupled Schottky diode in the dark and under deep UV (254 nm,

1.58 mW/cm^2) for different voltage biases at the third electrode (from 0 V to 9 V). In the dark, this device has low current in reverse bias and reaches milliamps in forward voltage bias, evidenced by the high rectification ratio of $1.76x10^7$ at ± 10 V and 9 V at the third electrode. This rectification ratio does not change significantly in the dark, even when varying voltages biases are applied at the third electrode. Furthermore, this increase in the level at the third electrode does not affect significantly the current in the reverse bias in the dark.

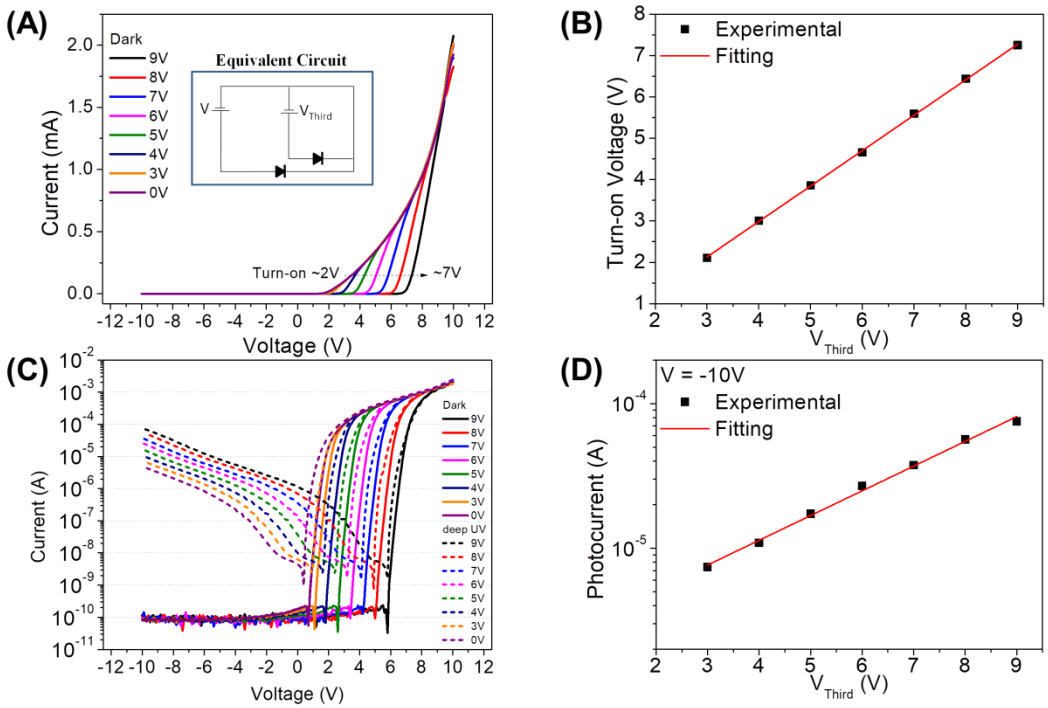

Fig. 3: a) I - V characteristics of the coupled Schottky diode in the dark under varying voltage biases at the third electrode with (inset) equivalent circuit of the coupled diode. b) Turn-on voltage versus voltage appied at the third electrode at V = −10 V. c) I - V characteristics of the coupled Schottky diode in the dark and under UV irradiation at different voltage biases at the third eletrode. (d) Photocurrent versus third electrode voltage at V = −10V.

Under UV irradiation, it is evident that the photocurrent increases significantly in the reverse bias leading to higher photocurrents. **Fig. 3d** shows that the logarithmic value of the photocurrent has increases linearly with V_{Third}, i.e. the coupled Schottky diode leads to increase the photocurrent, resulting in a much higher value than can be achieved from a Schottky diode. The photocurrent $(I_{uv} - I_{dk})$ at 254 nm, $V_{Third} = 9\,V$ and $V = -10\,V$ was 75.3 µA, which is 186 times greater than the photocurrent observed in the single Schottky diode reported in **Fig. 2**.

The internal electric potential difference is impacted by the presence of the third electrode which seems to shift the diode bias by an amount equal to the change in On-voltage. This is supported by **Fig. 4**, which presents a 2D simulation of the electric potential profile for the coupled Schottky diode at reverse bias. The third electrode creates a potential gradient between the Schottky and ohmic electrodes leading to an increased depletion region width and an increase in electron-hole pairs formation before they recombine. Thus, a higher voltage bias applied to the third electrode corresponds to greater efficiency in charge collection and, consequently, greater photocurrent.

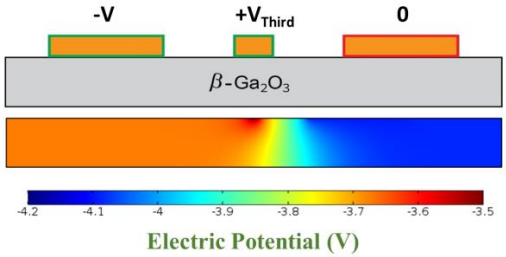

Fig. 4: 2D simulation of the electric potential profile for a coupled Schottky diode at reverse bias: V = −0.2 V and V_{third} = 1 V.

To evaluate the photoresponse, measurements were made in order to obtain the rise and decay time constants. **Fig. 5a** shows the current as a function of time measurements (*I-t*) for the coupled Schottky diode, with $V = -10\,V$, in the dark and under illumination, varying the level at the third electrode. To obtain the rise time constant, curves were fitted using by the following equation under UV light exposure:

$$I(t) = I_o + Ae^{-t/\tau_r}, \qquad (7)$$

where I_o and A are constants, t is the time, and τ_r is the rise time constant.

At $V_{third} = 0\,V$, the rise time was measured at 70.50 s. However, when the voltage at the third electrode was changed, not only does the photocurrent increase, but also it was possible to achieve faster rise times, with the fitted value for rise time being measured as 29.38 s at $V_{third} = 9\,V$. **Fig. 5b** summarizes the differences in the rise time and photocurrent as a function of the bias on V_{Third}; with the highest value of $V_{third}(9\,V)$, it is possible to achieve the shortest rise time constant and highest photocurrent, as highlighted in red. This change in time constant is also related to the change in the internal potential as illustrated in **Fig. 4**. When the electron-hole pair is formed by the incident deep UV irradiation and it is dissociated, those charges are accelerated by this potential resulting in performance improvements, i.e. a faster rise time and higher photocurrent. These improvements are proportional to the voltage level applied on the third electrode.

After the UV light is switched off, the current as a function of time (I-t) changes to a bi-exponential relationship. Likewise, the decay time constant was obtained for each curve, after turned-off the UV source, can be modeled using the following equation [24]:

$$I(t) = I_o + Ae^{-(t-t_o)/\tau_{d1}} + Be^{-(t-t_o)/\tau_{d2}}, \qquad (8)$$

where B and t_o are constants, τ_{d1} and τ_{d2} are the first and second decay time constant, respectively.

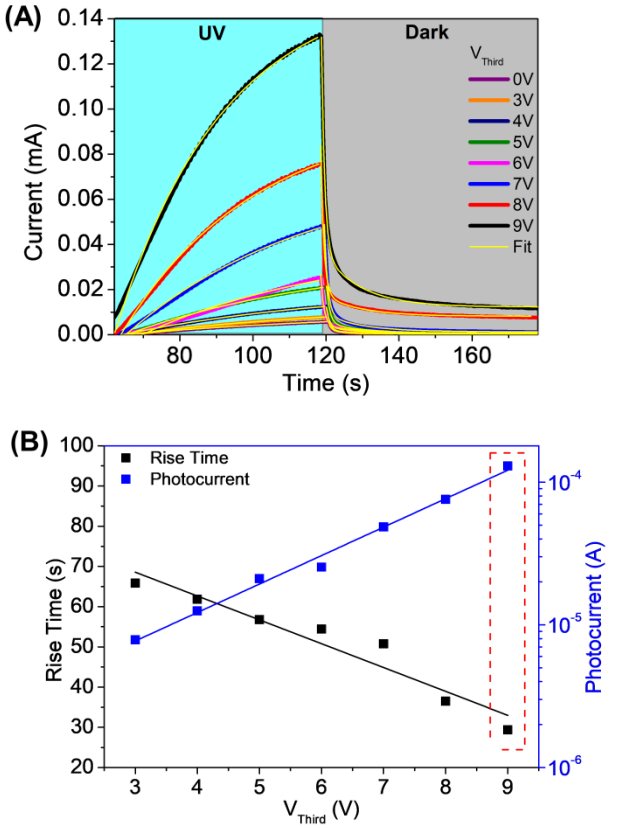

Fig 5: a) Rise and decay curves for photocurrent (I – t) of the coupled Schottky diode in the dark and under UV for different voltages bias at the third eletrode, and b) Rise time and photocurrent versus voltage at the third electrode.

The first decay time constant (τ_{d1}) was found to be 0.86 s, which probably relates to the recombination of the electrons formed in the conduction band with the holes from recombination centers present in the material, or from a band-to-band annihilation process [25]. The second time constant (τ_{d2}) was found to be 10.17 s, which is a much slower component and can be attributed to deep traps [25] that generates a persistent photocurrent effect [26]. Both rise and decay times do not change with the applied voltage at the third electrode.

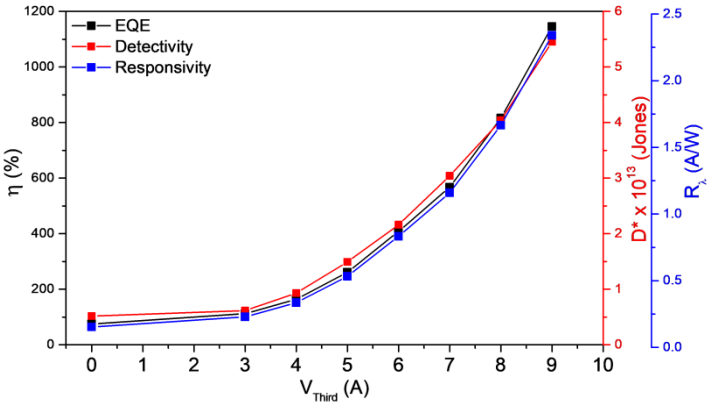

Fig. 6: Responsivity, external quantum efficiency (EQE/η) and detectivity as a function of third electrode voltage (V_{Third}) for the coupled Schottky diodes.

Overall, the coupled Schottky diodes showed an enhancement in the photodetector FOM. The responsivity and EQE of the conventional Schottky diode have presented 0.0125 A/W and 6.12 %, respectively. With the inclusion of the third electrode at $V_{third} = 0\,V$ bias, those values increased to 0.153 A/W and 74.88 %, respectively. However, by applying a greater voltage bias at the third electrode, the potential is enhanced increasing the photocurrent generation leading to higher values of both parameters, with maximum of 2.34 A/W and 1145.24% at $V_{third} = 9$ V, respectively. An EQE of more than 100% is often achieved in these devices if the internal gain increases with the voltage [27]. It can be related to changes in the depletion layer at the junction [28].

Fig. 6 shows the responsivity, EQE and detectivity as a function of the voltage bias on the third electrode. In terms of the detectivity, the conventional Schottky diode achieved a value of 1.02×10^{12} Jones that was improved to 5.18×10^{12} Jones for the coupled diode with $V_{third} = 0\,V$, which increased to 5.45×10^{13} Jones at $V_{third} = 9\,V$. The PDCR of the conventional Schottky diode was measured at 4.26×10^4 at 254 nm, that was improved to 6.09×10^4 for the coupled diode with $V_{Third} = 0\,V$ and $V = -10\,V$ and increased to $6.38x10^5$ when $V_{Third} = 9\,V$, which is a high light/dark ratio and represents an increase of one order of magnitude compared to the simple Schottky diode. The dark current has a negligible change during UV exposure from 10^{-11} to 10^{-10} A, which provides an attractive noise floor that is competitive with almost all UV detectors [24].

TABLE I:
COMPARISON OF THE PARAMETERS TO EVALUATE THE PERFORMANCE OF THE DEVICE AS DEEP UV PHOTODETECTOR WITH DIFFERENT VOLTAGE BIAS AT THE THIRD ELECTRODE.

	Conventional Schottky diode	**Coupled diode with $V_{Third} = 0\ V$**	**Coupled diode with $V_{Third} = 9\ V$**
Responsivity (A/W)	0.0125	0.153	2.34
EQE (%)	6.12	74.88	1145.24
Detectivity (Jones)	$1.02x10^{12}$	$5.18x10^{12}$	$5.45x10^{13}$
PDCR	$4.26x10^{4}$	$6.09x10^{4}$	$6.38x10^{5}$
I_{dk} reverse bias (A)	$1.0x10^{-11}$	$8.1x10^{-11}$	$1.1x10^{-10}$

Finally, we summarize the performance differences of the Schottky diode versus the coupled Schottky diode. **Tab I** provide a direct comparison of the control device (Schottky diode) versus the novel coupled-diode device reported in this paper. It is clear that the best performance is achieved using the coupled-diode device, in particular when the third terminal is biased to the highest possible voltage (in our case this was tested to $V_{Third} = 9\ V$). When comparing to the state of the art, Nakagomi *et al* [29] reported a diode with extremely low rise and decay time, but it responsivity was 0.053 A/W, which is better than our simple Schottky diode, but with the coupled Schottky diodes, we achieve a responsivity of 2.34 A/W. Kong *et al* [30] reported a high responsivity of 39.3 A/W, but it rise time was 95 s which compares unfavorably to our results 29.38 s. The FOMs that are most prominently above the state of the art are the PDCR and dark current reinforcing the fact that the coupling of two diodes is a promising result for deep UV sensor applications. Further studies should be conducted upon the coupled devices to measure the responsivity as a function of wavelength at similar deep UV radiation wavelengths; this might lead to higher responsivity values than those reported in this manuscript.

IV. CONCLUSION

The work reports the UV sensing behaviour of a β-Ga_2O_3-based coupled Schottky diode. This device exhibited good properties as rectification ratio, low dark current in reverse bias and a high forward current of 2 mA. The use of three terminals device instead of the conventional two terminals Schottky diode enables a substantial improvement in performance. The diodes shown high PDCR and high values of responsivity, EQE and detectivity. From the results, we confirm that this novel configuration of a coupled Schottky diode has enormous potential for deep UV sensor applications.

ACKNOWLEDGMENTS

The work was supported by the Solar Photovoltaic Academic Research Consortium II (SPARC II) project, gratefully funded by WEFO. The authors thank the Fundação de Amparo à Pesquisa do Estado de São Paulo (FAPESP) (Grant No. 2019/14366-3) and Programa de Pós-Graduação em Ciência e Tecnologia de Materiais (POSMAT) for technical and financial support.

REFERENCES

[1] 1. S. Nakagomi, T. Momo, S. Takahashi, and Y. Kokubun. Deep ultraviolet photodiodes based on β-Ga_2O_3/SiC heterojunction. Sensors Actuat A phys. July 2015, 232, 208-213. (10.1063/1.4818620)

[2] Y. Qin, S. Long, H. Dong, Q. He, G. Jian, Y. Zhang, X. Hou, P. Tan, Z. Zhang, H. Lv, Q. Liu, and M. Liu., Review of deep ultraviolet photodetector based on gallium oxide. Chinese Phys. B Jan 2019, 28, 1-17. (10.1088/1674-1056/28/1/018501)

[3] J. Yu, Z. Nie, L. Dong, L. Yuan, D. Li, Y. Huang, L. Zhang, Y. Zhang, and R. Jia, J. Influence of annealing temperature on structure and photoelectrical performance of β-Ga_2O_3/4H-SiC heterojunction photodetectors. J. Alloys Compd. Aug 2019, 798, 458–466. (10.1016/j.jallcom.2019.05.263)

[4] A. S. Pratiyush, Z. Xia, S. Kumar, Y. Zhang, and C. Joishi. MBE-Grown β-Ga_2O_3-Based Schottky UV-C Photodetectors With Rectification Ratio ~10^7. IEEE Photonics Technol. Lett. Oct 2018, 30, 2025–2028. (10.1109/LPT.2018.2874725)

[5] R. Pandeeswari and B. G. Jeyaprakash. High sensing response of β-Ga_2O_3 thin film towards ammonia vapours: Influencing factors at room temperature. Sensors Actuators B Chem. May 2014, 195, 206–214. (10.1016/j.snb.2014.01.025)

[6] M. Higashiwaki, K. Sasaki, A. Kuramata, T. Masui, and Y. Shigenobu. Gallium oxide (Ga_2O_3) metal-semiconductor field-effect transistors on single-crystal β-Ga_2O_3 (010) substrates. Appl. Phys. Lett. Jan 2012, 100, 1-3. (10.1063/1.3674287)

[7] X. Huiwen, H. Qiming, J. Guangzhong, L. Shibing, P. Tao, and L. Ming. An Overview of the Ultrawide Bandgap Ga_2O_3 Semiconductor Based Schottky Barrier Diode for Power Electronics Application. Nanoscale Res. Lett. Sept 2018, 13, 1-13. (10.1186/s11671-018-2712-1)

[8] A. Li, Q. Feng, J. Zhang, Z. Hu, Z. Feng, K. Zhang, C. Zhang, and H. Zhou. Investigation of temperature dependent electrical characteristics on Au/Ni/β-Ga_2O_3 Schottky diodes. Superlattices Microstruct. July 2018, 119, 212-217. (10.1016/j.spmi.2018.04.045)

[9] S. R. Thomas, G. Adamopoulos, Y. Lin, H. Faber, L. Sygellou, E. Stratakis, N. Pliatsikas, P. A. Patsalas, T. D. Anthopoulos, S. R. Thomas, G. Adamopoulos, Y. Lin, H. Faber, L. Sygellou, E. Stratakis, N. Pliatsikas, and P. A. Patsalas. High electron mobility thin-film transistors based on Ga_2O_3 grown by atmospheric ultrasonic spray pyrolysis at low temperatures. Appl. Phys. Lett. Aug 2014, 105, 1-5. (10.1063/1.4894643)

[10] T. Minami, Y. Nishi, and T. Miyata. Effect of the thin Ga_2O_3 layer in n^+-ZnO/n-Ga_2O_3/p-Cu_2O heterojunction solar cells. Thin Solid Films Dec 2013, 549, 65–69. (10.1016/j.tsf.2013.06.038)

[11] V. Vasanthi, M. Kottaisamy, K. Anitha, and V. Ramakrishnan. Near UV excitable warm white light emitting Zn doped γ-Ga_2O_3 nanoparticles for phosphor-converted White Light Emitting Diode. Ceram. Int. Feb 2019, 45, 2079-2087. (10.1016/j.ceramint.2018.10.111)

[12] X. C. Guo, N. H. Hao, D. Y. Guo, Z. P. Wu, Y. H. An, X. L. Chu, L. H. Li, P. G. Li, M. Lei, and W. H. Tang, J. β-Ga_2O_3/p-Si heterojunction solar-blind ultraviolet photodetector with enhanced photoelectric responsivity. J. Alloys Compd. Mar 2016, 660, 136–140. (10.1016/j.jallcom.2015.11.145)

[13] T. Oshima, M. Hashikawa, S. Tomizawa, K. Miki, T. Oishi, K. Sasaki, and A. Kuramata. β-Ga_2O_3-based metal-oxide-semiconductor photodiodes with HfO_2 as oxide. Appl. Phys. Express Nov 2018, 11, 1–4. (10.7567/APEX.11.112202)

[14] S. Oh, C. K. Kim, and J. Kim. High Responsivity β-Ga_2O_3 Metal-Semiconductor-Metal Solar-Blind Photodetectors with Ultraviolet Transparent Graphene Electrodes. ACS Photonics, Dec 2018, 5, 1123–1128. (10.1021/acsphotonics.7b01486)

[15] Z. Liu, X. Wang, Y. Liu, D. Guo, S. Li, Z. Yan, C. K. Tan, W. Li, P. Li, and W. Tang. A high-performance ultraviolet solar-blind photodetector based on a β-Ga_2O_3 Schottky photodiode. J. Mater. Chem. C Oct 2019, 7, 13920–13929. (10.1039/C9TC04912F)

[16] A. S. Pratiyush, S. Krishnamoorthy, R. Muralidharan, S. Rajan, and D. N. Nath. Advances in Ga_2O_3 solar-blind UV photodetectors. Gallium Oxide: Technology, Devices and Applications, Elsevier Inc. Oct 2018, pp 369-399. (10.1016/B978-0-12-814521-0.00016-6)

[17] C. Hou, R. M. Gazoni, R. J. Reeves, and M. W. Allen. Direct comparison of plain and oxidized metal Schottky contacts on β-Ga_2O_3. Appl. Phys. Lett. Jan 2019, 114, 1-5. (10.1063/1.5079423)

[18] Y. Yao, R. F. Davis, and L. M. Porter. Investigation of Different Metals as Ohmic Contacts to β-Ga_2O_3: Comparison and Analysis of Electrical Behavior, Morphology, and Other Physical Properties. J. Electron. Mater. Nov 2016, 46, 2053–2060. (10.1007/s11664-016-5121-1)

[19] J. Bae, H.-Y. Kim, and J. Kim. Contacting mechanically exfoliated β-Ga_2O_3 nanobelts for (opto)electronic device applications. ECS J. Solid State Sci. Technol. Dec 2017, 6, 3045–3048. (10.1149/2.0091702jss)

[20] L. A. M. Lyle, L. Jiang, K. K. Das, and L. M. Porter. Schottky contacts to β-Ga_2O_3. Gallium Oxide, Elsevier Inc., 2019, 231-261. (10.1016/B978-0-12-814521-0.00011-7)

[21] P. H. Carey, J. Yang, F. Ren, D. C. Hays, S. J. Pearton, S. Jang, A. Kuramata, and I. I. Kravchenko. Ohmic contacts on n-type β-Ga_2O_3 using AZO/Ti/Au. AIP Adv. Aug 2017, 7, 1–7. (10.1063/1.4996172)

[22] S. K. Cheung and N. W. Cheung. Extraction of Schottky diode parameters from forward current-voltage characteristics. Appl. Phys. Lett. June 1986, 49, 85–87. (10.1063/1.97359)

[23] K. Arora, N. Goel, M. Kumar, and M. Kumar. Ultrahigh Performance of Self-Powered β-Ga_2O_3 Thin Film Solar-Blind Photodetector Grown on Cost-Effective Si Substrate Using High-Temperature Seed Layer. ACS Photonics May 2018, 5, 2391–2401. (10.1021/acsphotonics.8b00174)

[24] P. Mukhopadhyay and W. V. Schoenfeld. High responsivity tin gallium oxide Schottky ultraviolet photodetectors. J. Vac. Sci. Technol. A Dec 2020, 38, 1-5. (10.1116/1.5128911)

[25] D. Guo, Z. Wu, P. Li, Y. An, H. Liu, X. Guo, H. Yan, G. Wang, C. Sun, L. Li, and W. Tang. Fabrication of β-Ga_2O_3 thin films and solarblind photodetectors by laser MBE technology. Opt. Mater. Express May 2014, 4, 1-10. (10.1364/OME.4.001067)

[26] Y. M. Lu, C. Li, X. H. Chen, S. Han, P. J. Cao, F. Jia, Y. X. Zeng, X. K. Liu, W. Y. Xu, W. J. Liu, and D. L. Zhu. Preparation of Ga_2O_3 thin film solar-blind photodetectors based on mixed-phase structure by pulsed laser deposition. Chinese Phys. B Jan 2019, 28, 1-7. (10.1088/1674-1056/28/1/018504)

[27] B. Zhao, F. Wang, H. Chen, Y. Wang, M. Jiang, X. Fang, and D. Zhao. Solar-Blind Avalanche Photodetector Based On Single ZnO−Ga_2O_3 Core−Shell Microwire. Nano Lett. May 2015, 15, 3988–3993. (10.1021/acs.nanolett.5b00906)

[28] S. Dhar, T. Majumder, P. Chakraborty, and S. P. Mondal. DMSO modified PEDOT:PSS polymer/ZnO nanorods Schottky junction ultraviolet photodetector: Photoresponse, external quantum efficiency, detectivity, and responsivity augmentation using N doped graphene quantum dots. Org. Electron. Feb 2018, 53, 101–110. (10.1016/j.orgel.2017.11.024)

[29] Nakagomi, T. Sakai, K. Kikuchi, and Y. Kokubun. β-Ga_2O_3/p-Type 4H-SiC Heterojunction Diodes and Applications to Deep-UV Photodiodes. Phys. Status Solidi Appl. Mater. Sci. Apr 2019, 216, 1–8. (10.1002/pssa.201700796)

[30] W. Y. Kong, G. A. Wu, K. Y. Wang, T. F. Zhang, Y. F. Zou, D. D. Wang, and L. B. Luo. Graphene-β-Ga_2O_3 heterojunction for highly sensitive deep UV photodetector application. Adv. Mater. Nov 2016, 28, 10725–10731. (10.1002/adma.201604049)